

Article

A Joint Estimation Method Based on Kalman Filter of Battery State of Charge and State of Health

Qingxia Yang ¹, Ke Ma ¹, Liyou Xu ¹, Lintao Song ¹, Xiuqing Li ^{2,*}  and Yefei Li ³

¹ College of Vehicle and Traffic Engineering, Henan University of Science and Technology, Luoyang 471023, China; qx_yang@sina.cn (Q.Y.); ma_ke6@163.com (K.M.); xlyou@haust.edu.cn (L.X.); song_strength@163.com (L.S.)

² National Joint Engineering Research Center for Abrasion Control and Molding of Metal Materials, Henan University of Science and Technology, Luoyang 471023, China

³ State Key Laboratory for Mechanical Behavior of Materials, Xi'an Jiaotong University, Xi'an 710049, China; liyefei@xjtu.edu.cn

* Correspondence: xqli@haust.edu.cn

Abstract: In a battery management system, the accurate estimation of the battery's state of health (SOH) and state of capacity (SOC) are vital functions. The traditional estimation methods have limitations. To accurately estimate the SOC and SOH of power battery and improve the performance of the long-term estimation of a battery's SOC, a joint estimation method based on a Kalman filter is proposed in this work. First, a second-order RC equivalent circuit model of a ternary lithium battery was built, whose parameters were identified online, and the model's accuracy was verified. Then, the battery data under actual working conditions were collected. The SOC and SOH were estimated based on the Kalman filter algorithm, and the simulation was implemented using MATLAB. Finally, according to a time scale transformation, the battery state was jointly estimated, the SOC was estimated at a short-time scale, the SOH was estimated at a long-time scale, and the SOH estimation results were updated to the model parameters for SOC estimation. The results show that the accuracy of the method is very good, and it can effectively improve estimation accuracy and ensure batteries' long-term estimation performance.

Keywords: ternary lithium battery; SOC; SOH; kalman filtering; battery management system



Citation: Yang, Q.; Ma, K.; Xu, L.; Song, L.; Li, X.; Li, Y. A Joint Estimation Method Based on Kalman Filter of Battery State of Charge and State of Health. *Coatings* **2022**, *12*, 1047. <https://doi.org/10.3390/coatings12081047>

Academic Editor: Je Moon Yun

Received: 22 June 2022

Accepted: 21 July 2022

Published: 24 July 2022

Publisher's Note: MDPI stays neutral with regard to jurisdictional claims in published maps and institutional affiliations.



Copyright: © 2022 by the authors. Licensee MDPI, Basel, Switzerland. This article is an open access article distributed under the terms and conditions of the Creative Commons Attribution (CC BY) license (<https://creativecommons.org/licenses/by/4.0/>).

1. Introduction

As the most promising energy source for electric vehicles and hybrid electric vehicles, lithium-ion batteries have many excellent characteristics including high energy density, a long cycle life, good working stability, and a wide range of operating temperatures. To ensure the safety and reliability of electric vehicles, a good battery management system is needed [1–5]. The accurate estimation of a battery's SOC and SOH is an important function of a battery management system [6–9], which can formulate a reasonable charge and discharge strategy for the vehicle, so that the battery can be fully and reasonably utilized and its service life can be extended. As a battery's SOC and SOH cannot be measured directly, they can be estimated based on the parameters that can be directly detected, such as the voltage, current, temperature, and so on [10,11].

With the continuous improvement and development of BMS technology, common battery SOC estimation methods include the charging state of capacity (SOC_{charge}) and the discharging state of capacity (SOC_{discharge}), and their advantages and disadvantages are as follows. The traditional SOC estimation methods mainly include the open circuit voltage method, ampere hour integration method, and so on [12–14]. The open-circuit voltage method presented by Zheng et al. [12] is simple and easy to use. However, this method is not suitable for an online calculation of a battery's SOC, because obtaining a battery's open-circuit voltage requires the battery to remain in a standing state for a long

time. In reference [13], Khalid et al. proposed a performance analysis of a commercial battery using a hardware-in-the-loop test-bed; as a result, the battery's voltage can be traced within a 0.04 V error after a long tracking period, and the battery's SOC can be estimated within 6% error based on an SOC-OCV method. The ampere-hour integral method proposed by Bao et al. [14] is simple in its calculation and easy to implement. However, this method heavily relies on a battery's initial SOC value, which is almost impossible to directly measure in vehicles. Data driven estimation methods mainly include neural network methods, support vector machines, and so on [15–17]; these methods are suitable for the SOC estimation of various batteries, establishing the mapping relationship between voltage, current, temperature, and SOC. In reference [17], Khalid et al. proposed a unified univariate-neural network model for a lithium-ion battery's SOC forecasting using a minimized Akaike information criterion algorithm, and the results showed that the SOC forecasting RMSE value can reach 3.236% using the AdaGrad optimizer evaluated with a computed C/10 rate SOC as the testing data. However, such methods have high requirements for large amounts of battery-related working data, and it is difficult to ensure the estimation performance under dynamic conditions. The methods based on an equivalent circuit model mainly include the Extended Kalman Filter (EKF), Unscented Kalman Filter (UKF), Particle Filter (PF), and so on [18–21]; as the battery is a nonlinear system, the EKF and UKF have certain limitations in dealing with nonlinear systems. The PF method has strong applicability to nonlinear systems, but there is the problem of particle degradation, which leads to the reduction of particle diversity and the reduction in the SOC calculation efficiency. Combining UKF with PF algorithms, this study proposed an unscented Kalman particle filter (UKPF) algorithm to improve SOC estimation accuracy, and updated particles are generated by a PF algorithm through UKF, which can effectively solve the particle degradation problem of the PF algorithm. Furthermore, the UKPF algorithm can overcome the problem of reducing the calculation accuracy due to the uncertainty of system noise in the use of UKF algorithm, which helps to overcome the problem of particle diversity reduction and SOC calculation efficiency reduction caused by particle degradation in the use of the PF algorithm.

In a long-term use process, the change of the SOH will lead to the change of the battery's internal characteristics, which should be considered when estimating the battery's SOC. So, the battery system parameters should be updated according to the SOH to achieve a joint state estimation, ensuring the accuracy and stability of long-term battery SOC estimation. One reference shows that a battery's SOC changes rapidly and its SOH changes slowly with time [1]. If the same time scale is used for a calculation, the computational demand for BMS is enormous. Therefore, the joint estimation of the battery state needs to be calculated on different time scales. Based on the dual UKF algorithm in reference [20], this study adopts the multi time scale joint estimation method of a UKPF-UKF algorithm, which can not only accurately estimate the SOC and SOH of the battery, but also improve the estimation accuracy and long-term estimation performance of the battery's SOC, and effectively reduce the amount of calculation for the system.

Aiming at the current joint estimation problem of battery states, this study adopts a joint estimation method of a battery's power state based on the Kalman filter. First, a second-order RC equivalent circuit model of a ternary lithium battery is introduced, whose parameters are identified online. Then, a battery's SOC was estimated using different methods, including the particle filter (PF), unscented Kalman filter (UKF), and unscented Kalman particle filter (UKPF). At the same time, the battery SOH was estimated by the unscented Kalman filter algorithm. Finally, the joint estimation of a battery's SOC and SOH was realized. The accuracy and validity of the proposed joint estimation of a battery's state were verified by experiments under actual working conditions.

2. Battery Modeling and Parameter Identification

2.1. Equivalent Circuit Model of Lithium Battery

To form a circuit network that describes a battery’s external characteristics, circuit components including capacitance, resistance, and constant voltage source are used by an equivalent circuit model, which has good applicability to various battery working states. The model state formulas, which are easy to analyze and apply, can be deduced.

The Rint model, Thevenin model, and PNGV model are common lithium battery equivalent circuit models. In these models, the Thevenin model is widely used due to its simple structure and good representation of the dynamic and external characteristics of lithium batteries [22]. Therefore, the Thevenin model was selected as the parameter identification model, which has a second-order RC. Figure 1 shows the block diagram of the Thevenin model, where U_{OC} represents the ideal voltage source, R_0 represents the battery’s ohmic resistance, U_1 is the voltage between R_1 and C_1 , U_2 is the voltage between R_2 and C_2 , R_1 and R_2 are the battery’s polarization resistance, C_1 and C_2 are the battery polarization capacitance, and U_T indicates battery terminal voltage. The system and observation equations can be obtained according to Kirchhoff’s law. The charging current is negative, and the discharge current direction is positive.

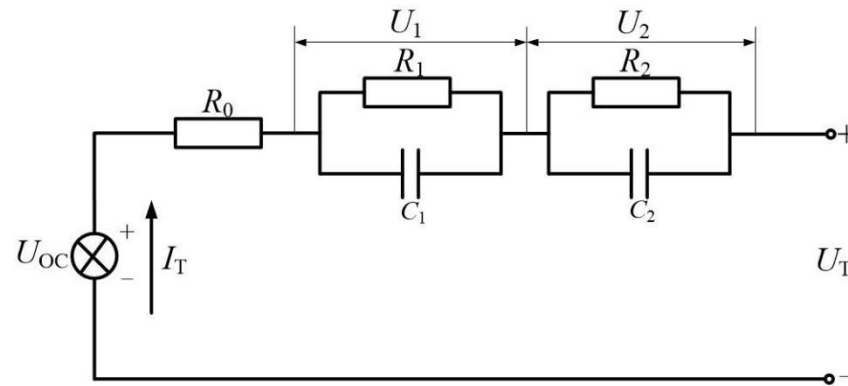


Figure 1. Second-order RC equivalent circuit model diagram.

System equation:

$$\begin{cases} \frac{dU_1}{dt} = -\frac{1}{R_1 C_1} U_1 + \frac{1}{C_1} I_T \\ \frac{dU_2}{dt} = -\frac{1}{R_2 C_2} U_2 + \frac{1}{C_2} I_T \\ \frac{dSOC}{dt} = -\frac{1}{Q_n} I_T \end{cases} \quad (1)$$

Observation equation:

$$U_T = U_{OC}(SOC) - R_0 I_T - U_1 - U_2 \quad (2)$$

2.2. Online Parameter Identification of Lithium Battery

To identify the model parameters, an INR18650-30Q ternary lithium battery was used for the test. The battery’s parameters are presented in Table 1.

Table 1. Parameters of INR18650-30Q battery.

Battery Parameters	Nominal Capacity (mAh)	Charge Cut-Off Voltage (V)	Discharge Cut-Off Voltage (V)	Nominal Voltage (V)
INR18650-30Q	3000	4.2	2.5	3.6

A battery’s offline parameter identification can only be identified under certain charging and discharging conditions, and a battery’s parameters will change with various internal and external factors during the working process, so a battery state’s parameters in actual operation cannot be obtained. Online parameter identification can identify battery

parameters in various working conditions, and the recursive least squares method can be used for battery online parameter identification [1].

Figure 2 shows the principle of lithium battery online parameter identification. When the battery is working, the working current $I(t)$ will be generated. After the working current passes through the battery, the terminal voltage $U(t)$ will be generated. The actual terminal voltage will be superimposed with a certain noise $n(t)$. When the working current passes through the battery model, it will calculate the terminal voltage $U_m(t)$. The terminal voltage $U_m(t)$ output of the model is different from the actual measured result $U(t)$ due to the inaccurate parameter identification, resulting in the errors $U_e(t)$ and $U_e(t) = |U(t) - U_m(t)|$. The error $U_e(t)$ was used to correct the model parameters through an identification algorithm (recursive least square algorithm). When the voltage $U(t)$ and $U_e(t)$ of the two terminals were very close, the battery model's online parameter identification results were finally obtained.

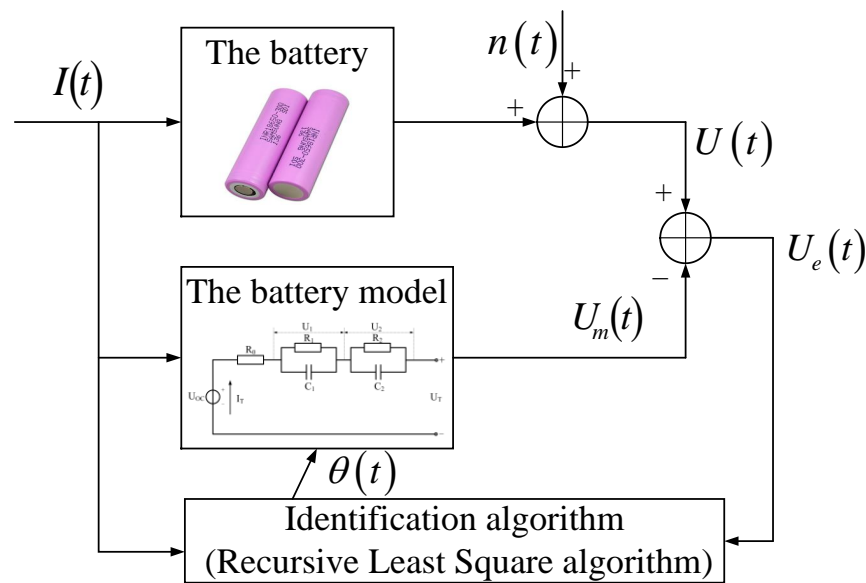


Figure 2. Schematic diagram of online parameter identification.

3. Joint State Estimation of Battery Power

3.1. UKF Algorithm Principle

The process of the unscented Kalman filter algorithm to estimate the system state is as follows:

- (1) Determine the state initial value x_0 and the initial value P_0 of the posterior state's error covariance.
- (2) Calculate the sampling points.

$$\begin{cases} x_k^0 = \hat{x}_k \\ x_k^i = x_k + \sqrt{(L + \lambda)P_{k-1}}, i = 1, 2, \dots, L \\ x_k^i = x_k - \sqrt{(L + \lambda)P_{k-1}}, i = L + 1, L + 2, \dots, 2L \end{cases} \quad (3)$$

where L is the state vector length, and L is 3 in this work.

The weight value can be computed as follows.

$$\begin{cases} \lambda = \alpha^2(L + k_i) - L \\ W_m^0 = \frac{\lambda}{L + \lambda}, W_m^i = \frac{1}{2(L + \lambda)}, i = 1, 2, \dots, 2L \\ W_c^0 = \frac{\lambda}{L + \lambda} + 1 - \alpha^2 + \beta, W_c^i = \frac{1}{2(L + \lambda)}, i = 1, 2, \dots, 2L \end{cases} \quad (4)$$

where $\alpha = 0.01$, $k_i = 0$, and $\beta = 2$.

(3) Update the prior state value \bar{x}_{k+1} and system variance predicted value P_{xx} .

$$\bar{x}_{k+1} = \sum_{i=0}^{2L} W_m^i x_k^i \quad (5)$$

$$P_{xx} = \sum_{i=0}^{2L} (W_c^i (x_k^i - \bar{x}_{k+1})(x_k^i - \bar{x}_{k+1})^T) + Q_k \quad (6)$$

where Q_k is the system noise covariance matrix.

(4) Update the observed value \hat{y}_{k+1} and predicted value P_{yy} of the observed variance.

$$\hat{y}_{k+1} = \sum_{i=0}^{2L} W_m^i y_k^i \quad (7)$$

$$P_{yy} = \sum_{i=0}^{2L} (W_c^i (y_k^i - \hat{y}_{k+1})(y_k^i - \hat{y}_{k+1})^T) + R_k \quad (8)$$

Update the covariance P_{xy} , posterior state value \hat{x}_{k+1} , and posterior state error covariance P_k .

$$P_{xy} = \sum_{i=0}^{2L} W_c^i (x_k^i - \bar{x}_{k+1})(y_k^i - \hat{y}_{k+1})^T \quad (9)$$

$$K_k = \frac{P_{xy}}{P_{yy}} \quad (10)$$

$$\hat{x}_{k+1} = \bar{x}_{k+1} + K_k (y_{k+1} - \hat{y}_{k+1}) \quad (11)$$

$$P_k = P_{xx} - K_k P_{xy}^T \quad (12)$$

3.2. UKPF Algorithm Principle

(1) PF algorithm principle

The basic idea of particle filtering is to first extract some discrete random particles, then adjust the weight and particle position based on the state observation, and then use these samples to approximate the posterior state distribution. These particles use a probability density function to estimate the mean of the sample.

The process of the system state estimation via the particle filter algorithm is as follows:

(1) Initialization:

A priori probability $P(x_0)$ is used to generate N SOC initial particles $\{SOC_0^i\}_{i=1}^N$ with particle weight $\{q_0^i\}_{i=1}^N = 1/N$.

(2) Cyclic calculation:

a. Update particle weight;

$$\begin{cases} w_k^i = w_{k-1}^i p(U_{L(k)} | SOC_k^i) = w_k^i \\ p[U_{L(k)} - h(SOC_k^i)], i = 1, 2, \dots, N \end{cases} \quad (13)$$

b. Normalize weights;

$$w_k^i = w_k^i / \sum_{i=1}^N w_k^i \quad (14)$$

c. Calculate the least mean square estimate;

$$\tilde{SOC}_k \approx \sum_{i=1}^N (w_k^i \times SOC_k^i) \quad (15)$$

d. Resampling: effective particle number $N_{\text{eff}} = 1 / \sum_{i=1}^N (w_k^i)^2$, when $N_{\text{eff}} \leq N_s$, particles are set from the obtained $\{SOC_k^i, i = 0, 1, 2, \dots, N\}$;

e. Prediction: The unknown parameter SOC_{k+1}^i is predicted by the equation of the state;

f. Judge the end condition of the program. At the moment $k = k + 1$, if the calculation result does not reach the pre-set precision requirement, the program jumps to step a.

(2) UKPF algorithm principle

When the particle filter is applied to estimate the system state, it has the problems of a low efficiency and poor accuracy, due to the imbalance caused by the different particle weights. This paper uses the combination of the unscented Kalman filter and particle filter algorithms for estimation, as the following steps:

(1) Initialization:

The initial particle set is generated by sampling according to the prior probability $P(x_0)$.

$$x_k(i) \sim p\{x_k|x_{k-1}(i)\}, i = 1, 2, \dots, N \tag{16}$$

(2) Update:

The UKF algorithm is used to update the mean and variance of each independent particle to update the particle set. The following is the calculation process:

a. Given the initial estimation and variance of the system state \hat{x}_0, P_0 , proceed with the dimensional expansion processing and obtain $\hat{x}_0 = [\hat{x}_0^T \ 0 \ 0]^T, P_0 = \text{diag}[P_0 \ Q \ R]$.

b. Calculate the set of Sigma points: $k = 1, 2, \dots, N$

$$\begin{cases} x_{k-1}^0 = \hat{x}_{k-1}, & i = 0 \\ x_{k-1}^i = \hat{x}_{k-1} + \left(\sqrt{(n+\lambda)P_{k-1}}\right)_i, & i = 1, 2, \dots, n \\ x_{k-1}^i = \hat{x}_{k-1} - \left(\sqrt{(n+\lambda)P_{k-1}}\right)_i, & i = n+1, n+2, \dots, 2n \end{cases} \tag{17}$$

where P is the covariance; n is the state variable dimension, $n = 3$; and λ is the proportional coefficient, and it is determined according to the actual situation.

c. Time prediction: covariance matrix of variables and one-step prediction can be obtained according to the state space model of system:

$$\begin{cases} c_{k|k-1}^i = f(c_{k-1}^i) \\ \hat{x}_{k|k-1} = \sum_{i=0}^{2n} W_i^m c_{k|k-1}^i \\ P_{x,k|k-1} = \sum_{i=0}^{2n} W_i^c (c_{k|k-1}^i - \hat{x}_{k|k-1})(c_{k|k-1}^i - \hat{x}_{k|k-1})^T + Q_k \\ g_{k|k-1}^i = h(c_{k|k-1}^i) \\ \hat{y}_{k|k-1} = \sum_{i=0}^{2n} W_i^m g_{k|k-1}^i \end{cases} \tag{18}$$

d. Measure the update—modify the state predictions with the latest observations:

$$\begin{cases} P_{y,k} = \sum_{i=0}^{2n} W_i^c (g_{k|k-1}^i - \hat{y}_{k|k-1})(g_{k|k-1}^i - \hat{y}_{k|k-1})^T + R_k \\ P_{xy,k} = \sum_{i=0}^{2n} W_i^c (c_{k|k-1}^i - \hat{x}_{k|k-1})(g_{k|k-1}^i - \hat{y}_{k|k-1}) \\ K = P_{xy,k} P_{y,k}^{-1} \\ \hat{x}_k = \hat{x}_{k|k-1} + K(y_k - \hat{y}_{k|k-1}) \\ P_{x,k} = P_{x,k|k-1} - K P_{y,k} K^T \end{cases} \tag{19}$$

(3) Importance sampling:

According to the result of step (2), the suggested distribution function is obtained:

$$x_k^i \sim q(x_k^i | x_{k-1}^i, Z_k) = N(\hat{x}_k^i, \hat{P}_k^i), i = 1, 2, \dots, N \quad (20)$$

Sample particles from the proposed distribution function, calculate the weight of the particles, and then normalize.

(4) Resampling:

Resample the particle set and redistribute the weight of the particles to obtain a new supporting particle set:

$$\{\hat{x}_k^j, 1/N; j = 1, 2, \dots, N\} \quad (21)$$

(5) Return step (2), the algorithm ends.

3.3. Multi-Time Scale Joint Estimation of Battery power State

Figure 3 shows a multi-time scale joint estimation method of a battery’s power state, in which the parameter identification, UKF, and UKPF are main components. When the battery power is working, a battery’s SOC changes quickly and its SOH changes slowly. Therefore, the estimated battery state should be updated at a high frequency, whereas the SOH should be updated at a fixed frequency. If the SOC and SOH are estimated using the same update frequency, it will greatly increase the amount of system calculations.

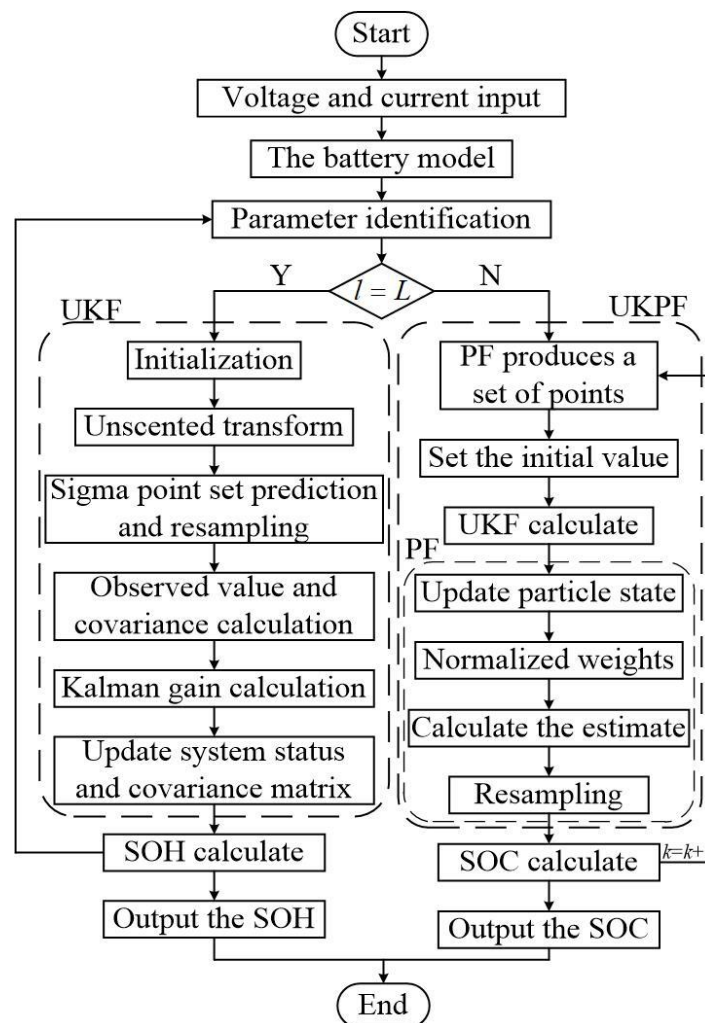


Figure 3. Flow chart of multi-time scale joint estimation method.

The micro estimated SOC based on UKPF and the macro estimated SOH based on UKF were set for the joint estimation of a battery's power state at multiple time scales. Set the time scale transformation L . If the time scale does not reach the set scale change L , the UKPF cycle calculation of SOC is carried out; otherwise, the UKF calculation of SOH is carried out once. Meanwhile, the SOH estimates are updated with the system parameters and applied to the SOC estimates.

The specific steps of the multi-time scale joint estimation of battery power status are as follows:

- (1) Input the battery voltage and current data into the battery model for online parameter identification;
- (2) Determine whether the time scale transformation is met, if so, step (3) is carried out, otherwise, step (4) is carried out;
- (3) UKF estimates SOH and uses estimated results to update system parameters;
- (4) UKPF cycle estimation SOC;
- (5) Output the SOC and SOH estimation results.

4. Test Results and Analysis

4.1. Test Platform Building and Test Data Collection

To make the collected test data valid, a battery charge and discharge test system (Figure 4) is established, including a host computer, battery test system, and an environmental test chamber. The battery detection system is responsible for charging and discharging the battery through the control signal of the upper computer, and the battery data collected will be uploaded to the upper computer. The environmental test chamber provides a suitable environment for battery testing, including temperature and relative humidity.

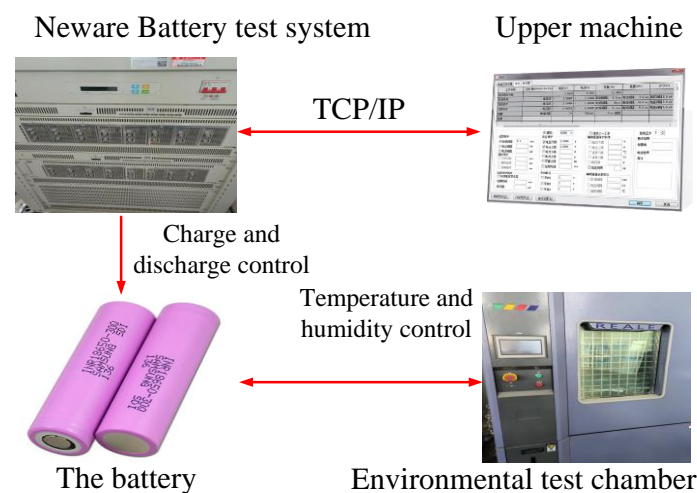


Figure 4. Battery charge and discharge test system.

The Urban Dynamometer Driving Schedule (UDDS) condition was used for data collection, and the battery voltage and current data were collected for 24,000 s, which are shown in Figure 5. The test temperature was set at 25 °C, relative humidity was set at 40%, initial voltage was 4.2 V, end voltage was 2.5 V, sampling interval was 0.1 s, and the discharge capacity attenuation rate was 100%.

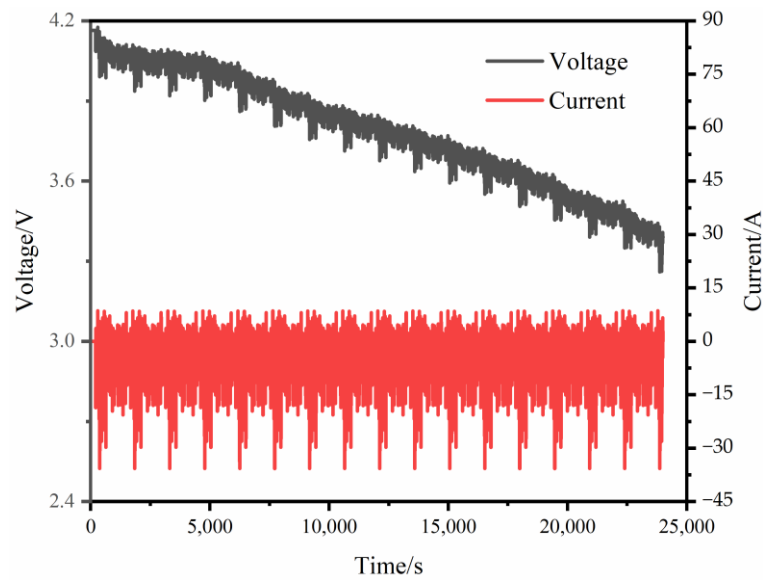


Figure 5. UDDS working voltage and current diagram.

4.2. Parameter Identification Results

Figures 6 and 7 are the terminal voltages and errors identified online by collecting the voltage and current of the battery at 24,000 s UDDS discharge. The model value of the battery’s terminal voltage basically agrees with the actual value as shown in Figure 6. At the beginning of the parameter identification, the model terminal voltage rapidly converges to the real value, and the model terminal voltage always maintains a good tracking effect compared to the real value within the 0.04V error, as shown in Figure 7. The results indicate that the established model can be used to describe the dynamic change process of battery power.

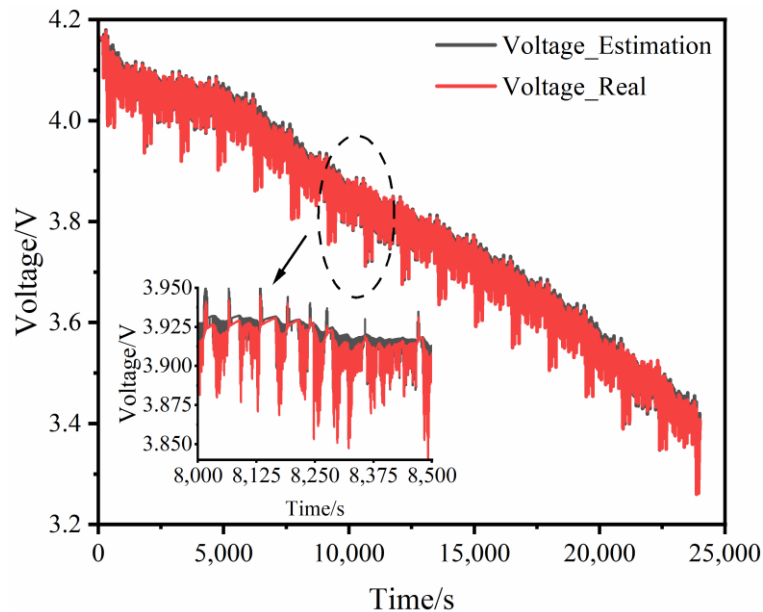


Figure 6. Battery terminal voltage diagram.

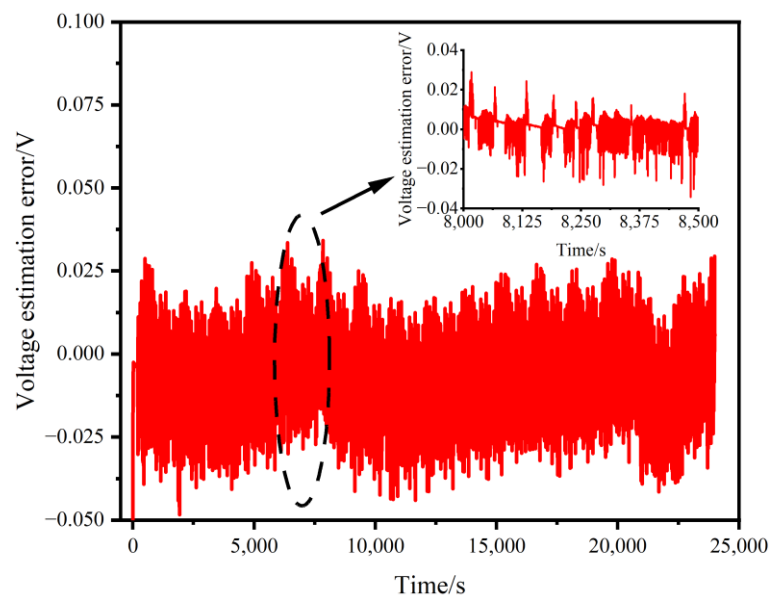


Figure 7. Battery terminal voltage error diagram.

The online parameters were identified every 6 s in the UDDS discharge condition for 24,000 s, and the identification results based on the recursive least squares method are shown in Figures 8 and 9, in which the X-axis represents the number of iterations of parameter identification and the Y-axis represents the identification results of the ohmic internal resistance and RC loop parameters. It can be seen from Figure 8 that R_0 decreases rapidly at the beginning, reaches the lowest value near the 1200th iteration, and then gradually becomes stable. References [23,24] show that the ohmic resistance decreases with the increase of the battery temperature, and the ohmic resistance increases with the decrease of the battery's SOC. During use, the internal temperature of a battery increases and the R_0 estimate decreases. With the increase of time, the internal and external temperature of the battery balances, and the R_0 estimate result tends to be stable. Accompanying the discharge process, the battery's SOC decreases and the value of estimated R_0 increases. It is highly consistent with the conclusion that the ohmic resistance decreases with an increasing battery temperature, but it increases with the decrease of SOC.

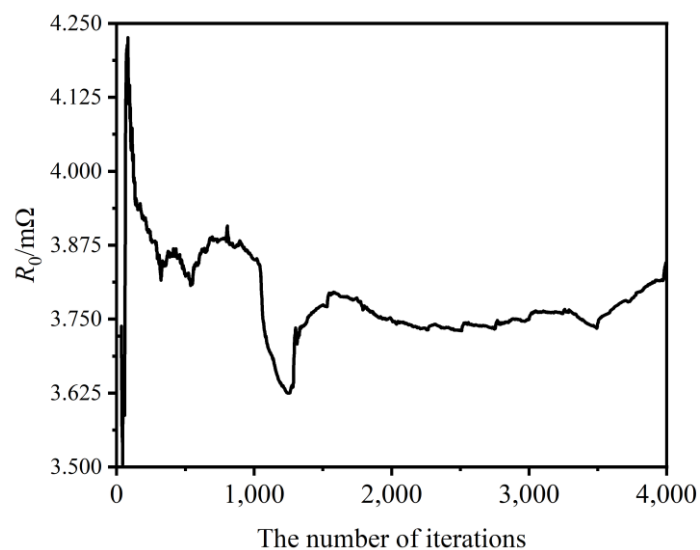


Figure 8. R_0 identification result diagram.

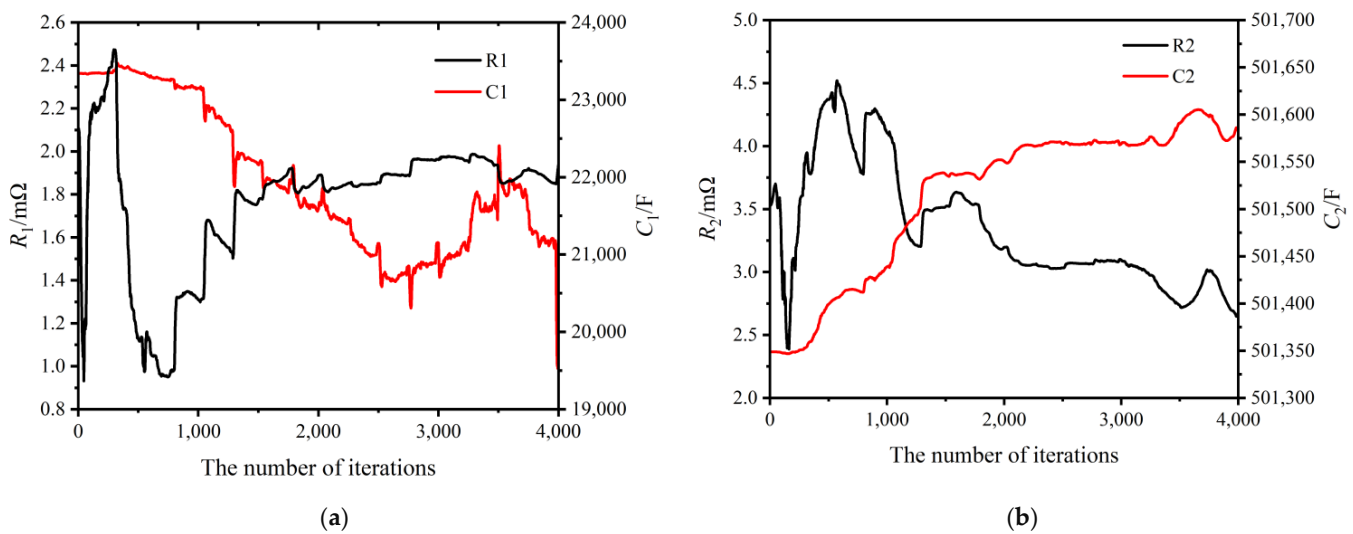


Figure 9. RC loop identification result: (a) R_1 , C_1 ; (b) R_2 , C_2 .

In the initial stage of parameter identification, the large variation range of the parameters is caused by the large difference between the set initial value and the actual value. The identification values of each parameter tend to be stable, and the identification results are accurate. The product of R_1C_1 is smaller than the product of R_2C_2 (Figure 9), which is consistent with the actual discharge characteristics of the battery. The results also further verify the model's reliability and the parameter identification accuracy.

4.3. Multi-Time Scale Joint Estimation Results

(1) UKPF algorithm estimation of SOC

To verify the validity and accuracy of the UKPF-based charge state estimation, the results of the UKPF-based charge state estimation were compared with those of the other two algorithms based on the PF and UKF algorithms.

The experimental data measured in the UDSS conditions were used for a simulation in MATLAB. Figure 10 shows the SOC_discharge estimation results based on the three algorithms when the SOC value ranges from 1 to 0.2. When estimating a battery's SOC_discharge, the estimated results of the three algorithms can be adequately used to trace the changes of the real value, as shown in Figure 10a. Compared with the SOC_discharge's estimated results of the UKF and PF, the estimated results of the UKPF are much more realistically close to the real value. The SOC_discharge estimation errors of the UKF and PF fluctuate greatly, and the stability is weaker than that of the UKPF algorithm, as shown in Figure 10b. Combining the UKF with the PF, the UKPF algorithm proposed in this paper can ensure the diversity of particles, and improve the estimation accuracy and stability of the PF algorithm, which can effectively solve the particle degradation problem of the PF algorithm in reference [1]. Furthermore, the UKPF algorithm can overcome the problem of accurately reducing the calculation accuracy due to the uncertainty of system noise in the use of the UKF algorithm in reference [2], which helps to overcome the problem of particle diversity reduction and the SOC calculation efficiency reduction caused by the particle degradation with the use of the PF algorithm. As SOC_discharge estimation algorithms are based on the method of data processing, the method is also applicable to the estimation of the SOC in the charging process. Therefore, when estimating a battery's SOC, fast convergence, a high estimation accuracy, and strong anti-interference ability are the advantages of the UKPF algorithm.

(2) UKF algorithm estimation of SOH

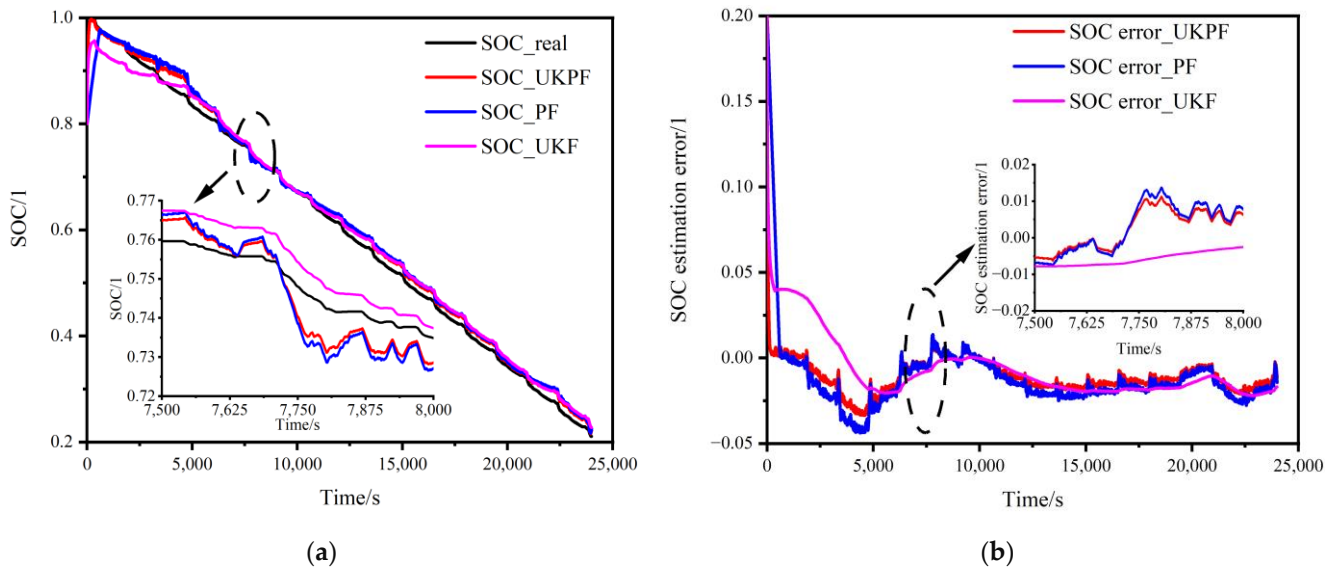


Figure 10. Result of SOC_discharge simulation based on different algorithms. (a) SOC_discharge estimation based on the UKPF, PF and UKF algorithms; (b) SOC_discharge estimation error based on the UKPF, PF and UKF algorithms.

To verify the validity and accuracy of the SOH estimation based on the UKF, UDDS test conditions were used for verification. Figure 11 gives the results and the SOH error. When the UKF algorithm estimates the battery’s SOH, the estimation result basically fluctuates around the true value, as shown in Figure 11a. In the early stage, the SOH estimates have a smaller range of fluctuations. However, in the middle and late stages, the SOH estimates fluctuate greatly. The error value of the UKF’s SOH estimation is within 2.5% (see Figure 11b). Its battery discharge characteristics are good in the early stage, so the SOH error is small, but it gradually increases in the middle and late stages, corresponding to the battery’s SOC. Therefore, the UKF algorithm can effectively estimate the SOH of a lithium-ion battery.

(3) Multi-time scale joint estimation results

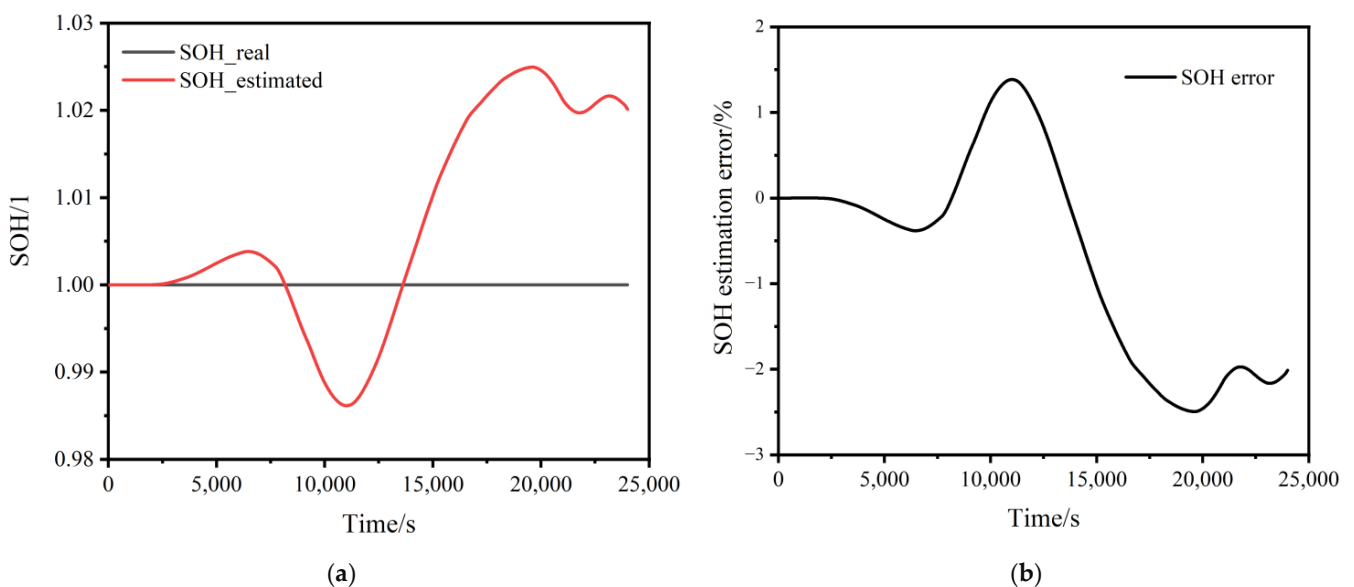


Figure 11. The result of SOH estimation: (a) SOH estimation; (b) SOH estimation error.

To verify the accuracy and validity of the multi-time scale joint estimation, after SOC is estimated 60 times, the SOH is estimated once, and the battery capacity is corrected once

using the estimated SOH. The time scale transformation of SOH estimation is 6000 ms, and the step length of SOC_discharge estimation is 100 ms. Figure 12 shows the results of the multi-time scale joint estimation.

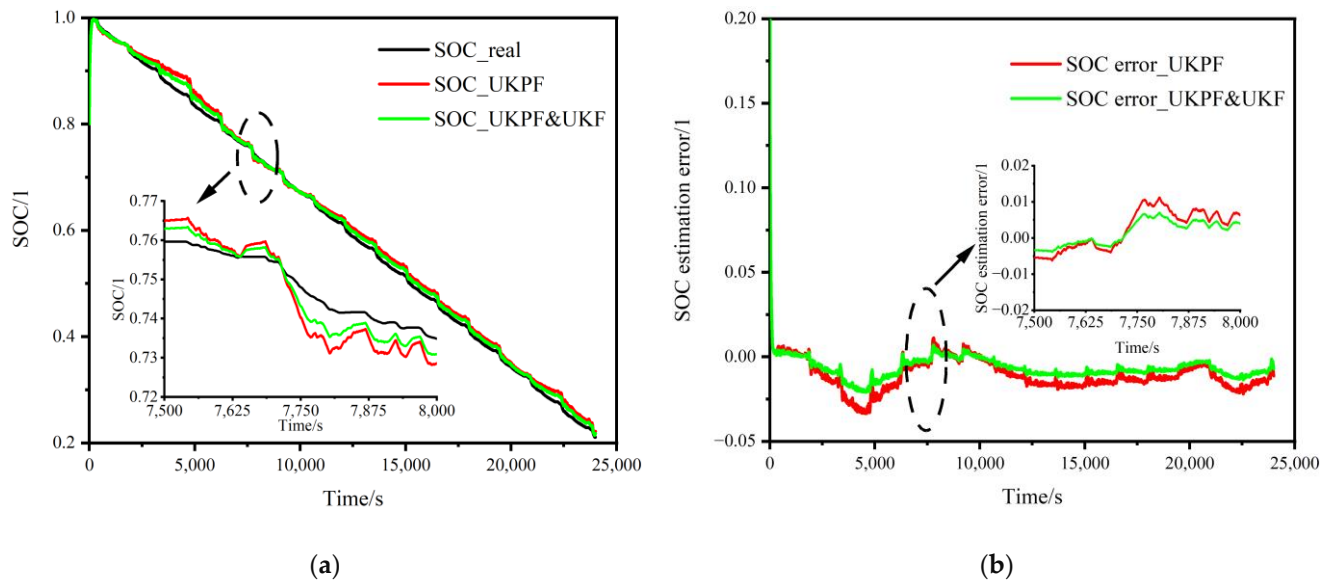


Figure 12. Joint estimation simulation graph. (a) SOC_discharge estimation based on the UKPF and multi-time scale joint estimation algorithms; (b) SOC_discharge estimation error based on the UKPF and multi-time scale joint estimation algorithms.

Both joint estimation and the UKPF can quickly converge from the set initial value to a position close to the true value, as shown in Figure 12a. During the entire estimation process, the joint estimation results are closer to the real value, and the joint estimation results still have high accuracy (within 2.2% estimation error) when the battery discharge characteristics are poor at the end of the discharge, as shown in Figure 12b. It is also evident from Figure 12b that the fluctuation range of the joint estimation error is small, and the overall error value is smaller than that of the UKPF algorithm. The average error and maximum error of the joint estimation algorithm for the SOC_discharge are both smaller than those of the UKPF algorithm, as shown in Table 2, and the SOC-estimated mean error based on the joint estimation algorithm can reach 0.74%. Therefore, the multi-time scale joint estimation method based on the data processing method can not only accurately estimate SOH, but also has good estimation performance for a battery's SOC.

Table 2. SOC estimated results.

SOC Estimated Method	SOC Estimated Mean Error	SOC Estimated MAXIMUM error
Joint estimation algorithm	0.74%	2.11%
UKPF algorithm	1.19%	3.37%

5. Conclusions

A multi-time scale joint state estimation method for a ternary lithium battery was proposed. A second order RC equivalent circuit model of a lithium battery was established, and the identification results were imported into the algorithm to realize online parameter identification. The UKPF method was used to estimate the SOC and SOH, and the UKF was used to estimate the SOH. The joint estimation was realized by time scale transformation. Simulation experiments were carried out in MATLAB.

- (1) The battery parameters can be identified online. The error of the parameter identification results is less than 5%, which verifies the validity and accuracy of the model.

Therefore, this model can accurately represent the working process of a lithium battery and lays a foundation for the subsequent estimation of its battery state.

- (2) Compared with the UKF and the PF algorithm, the UKPF algorithm has higher robust accuracy and stability, and its estimation error of a lithium battery's state of charge is less than 3.4%. The SOH error of the UKF algorithm is less than 2.5%, which can accurately and effectively estimate the SOH of the battery.
- (3) The multi-time scale joint estimation error is within 2.2%, which significantly improves the estimation accuracy of a battery's SOC and ensures the long-term estimation performance of a battery.

In this study, a battery's state of charge and health are estimated based on some battery parallel experiments. However, in electric vehicles, power batteries are usually used in series and parallel groups; therefore, in future research, discussion should focus on determining if the estimation methods proposed in this study are still valid while the battery (pack) configuration and cell chemistry change, and relevant experiments should be further improved in the future. Moreover, as the variation of temperature has a significant impact on the battery's parameters, the variation in temperature should be considered to ensure a better accuracy in real-life applications. In addition, the variation of temperature should be taken as an important factor in the battery state estimation in future works.

Author Contributions: Q.Y.: Writing—original draft, Conceptualization, Software, Data curation. K.M.: Visualization, Investigation. L.X.: Writing—review & editing, Software. L.S.: Investigation. X.L.: Supervision, Methodology. Y.L.: Software. All authors have read and agreed to the published version of the manuscript.

Funding: The study was supported by the Scientific Research Staring Foundation for Doctor of Henan University of Science and Technology, China (Grant no. 13480045), and Henan University of Science and Technology 2021 Young Backbone Teacher Training Program. In addition, we want to thank the support from the Provincial and Ministerial Collaborative Innovation Center of Non-ferrous Metal New Materials and Advanced Processing Technology.

Institutional Review Board Statement: Not applicable.

Informed Consent Statement: Not applicable.

Data Availability Statement: Not applicable.

Conflicts of Interest: The authors declare no conflict of interest.

References

1. Yang, Q.; Xu, J.; Li, X.; Xu, D.; Cao, B. State-of-health estimation of lithium-ion battery based on fractional impedance model and interval capacity. *Int. J. Electr. Power Energy Syst.* **2020**, *119*, 105883. [[CrossRef](#)]
2. Xiao, F.; Li, C.; Fan, Y.; Yang, G.; Tang, X. State of charge estimation for lithium-ion battery based on Gaussian process regression with deep recurrent kernel. *Int. J. Electr. Power Energy Syst.* **2020**, *124*, 106369. [[CrossRef](#)]
3. Wang, B.; Xuan, D.; Zhao, X.; Chen, J.; Lu, C. Dynamic battery equalization scheme of multi-cell lithium-ion battery pack based on PSO and VUFLC. *Int. J. Electr. Power Energy Syst.* **2021**, *136*, 107760. [[CrossRef](#)]
4. Trovò, A.; Saccardo, A.; Giomo, M.; Guarnieri, M. Thermal modeling of industrial-scale vanadium redox flow batteries in high-current operations. *J. Power Sources* **2019**, *424*, 204–214. [[CrossRef](#)]
5. Deja, P.; Kurpiel, W. Systems for Protecting and Controlling the Lithium Cells. *ECS Trans.* **2019**, *95*, 337–347. [[CrossRef](#)]
6. Sung, W.; Lee, J. Improved capacity estimation technique for the battery management systems of electric vehicles using the fixed-point iteration method. *Comput. Chem. Eng.* **2018**, *117*, 283–290. [[CrossRef](#)]
7. Zhang, Y.B.; Zhang, H.T. Design and Application of Lithium-ion Battery Management System: Review of New Energy Technology and Power Management. *Cell* **2020**, *50*, 105–106.
8. Moura, S.J.; Argomedeo, F.B.; Klein, R.; Mirtabatabaei, A.; Krstic, M. Battery State Estimation for a Single Particle Model with Electrolyte Dynamics. *IEEE Trans. Control. Syst. Technol.* **2017**, *25*, 453–468. [[CrossRef](#)]
9. Lu, J.; Wei, L.; Pour, M.M.; Mekonnen, Y.; Sarwat, A.I. Modeling discharge characteristics for predicting battery remaining life. In Proceedings of the 2017 IEEE Transportation Electrification Conference and Expo (ITEC), Chicago, IL, USA, 22–24 June 2017.
10. Misyris, G.S. State-of-charge estimation for li-ion batteries: A more accurate hybrid approach. *IEEE Trans. Energy Convers.* **2019**, *34*, 109–119. [[CrossRef](#)]

11. Mandli, A.R. Fast computational framework for optimal life management of lithium-ion batteries. *Int. J. Energy Res.* **2018**, *42*, 1973–1982. [[CrossRef](#)]
12. Zheng, F.; Xing, Y.; Jiang, J.; Sun, B.; Kim, J.; Pecht, M. Influence of different open circuit voltage tests on state of charge online estimation for lithium-ion batteries. *Appl. Energy* **2016**, *183*, 513–525. [[CrossRef](#)]
13. Khalid, A.; Stevenson, A.; Sarwat, A.I. Performance Analysis of Commercial Passive Balancing Battery Management System Operation Using a Hardware-in-the-Loop Testbed. *Energies* **2021**, *14*, 8037. [[CrossRef](#)]
14. Bao, H.; Yu, Y. Error Correction of Battery SOC Estimation Based on Ampere-hour Integral Method. *Comput. Simul.* **2013**, *30*, 148–151.
15. Chen, J.; Ouyang, Q.; Xu, C.; Su, H. Neural network based state of charge observer design for lithium-ion batteries. *IEEE Trans. Control. Syst. Technol.* **2017**, *26*, 1–9. [[CrossRef](#)]
16. Guo, G.F.; Shui, L.; Wu, X.L.; Cao, B.G. SOC Estimation for Li-Ion battery using svm based on particle swarm optimization. *Adv. Mater. Res.* **2014**, *1051*, 1004–1008. [[CrossRef](#)]
17. Khalid, A.; Sarwat, A.I. Unified Univariate-Neural Network Models for Lithium-Ion Battery State-of-Charge Forecasting Using Minimized Akaike Information Criterion Algorithm. *IEEE Access* **2021**, *9*, 39154–39170. [[CrossRef](#)]
18. Afshar, S.; Morris, K.; Khajepour, A. State-of-charge estimation using an EKF-based adaptive observer. *IEEE Trans. Control. Syst. Technol.* **2019**, *27*, 1907–1923. [[CrossRef](#)]
19. Jiang, C.; Taylor, A.; Duan, C.; Bai, K. Extended Kalman Filter based battery state of charge (SOC) estimation for electric vehicles. In Proceedings of the IEEE Transportation Electrification Conference and Expo, Detroit, MI, USA, 16–19 June 2013; pp. 1–5.
20. Shi, P.; Zhao, Y.W. Application of unscented Kalman filter in the SOC estimation of Li-ion battery for autonomous mobile robot. In Proceedings of the IEEE International Conference on Information Acquisition, Weihai, China, 20–23 August 2006; pp. 1279–1283.
21. Xia, B.; Sun, Z.; Zhang, R.; Cui, D.; Lao, Z.; Wang, W.; Sun, W.; Lai, Y.; Wang, M. A comparative study of three improved algorithms based on particle filter algorithms in SOC estimation of lithium-ion batteries. *Energies* **2017**, *10*, 114901–114914. [[CrossRef](#)]
22. Kurpiel, W.; Deja, P.; Polnik, B.; Skóra, M.; Miedziński, B.; Habrych, M.; Debita, G.; Zamłyńska, M.; Falkowski-Gilski, P. Performance of Passive and Active Balancing Systems of Lithium Batteries in Onerous Mine Environment. *Energies* **2021**, *14*, 7624. [[CrossRef](#)]
23. Wei, K.; Chen, Q.Y. States Estimation of Li-ion Power Batteries Based on Adaptive Unscented Kalman Filters. In Proceedings of the CSEE, Klagenfurt, Austria, 23–25 April 2014; pp. 445–452.
24. Remmlinger, J.; Buchholz, M.; Meiler, M.; Bernreuter, P.; Dietmayer, K. State-of-health monitoring of lithium-ion batteries in electric vehicles by on-board internal resistance estimation. *J. Power Sources* **2011**, *196*, 5357–5363. [[CrossRef](#)]